Journal of Catalysis 266 (2009) 299–307

Contents lists available at ScienceDirect

Journal of Catalysis

journal homepage: www.elsevier.com/locate/jcat

Stable active oxygen on mesoporous Au/TiO_2 supported catalysts and its correlation with the CO oxidation activity

A. Tost, D. Widmann, R.J. Behm *

Institute of Surface Chemistry and Catalysis, University Ulm, D-89069 Ulm, Germany

ARTICLE INFO

Article history:
Received 15 May 2009
Revised 22 June 2009
Accepted 23 June 2009
Available online 22 July 2009

Keywords:
Mesoporous Au/TiO_2
CO oxidation
Oxygen storage capacity (OSC)
Temporal analysis of products (TAP)

ABSTRACT

Following the recent finding [M. Kotobuki, R. Leppelt, D. Hansgen, D. Widmann, R.J. Behm, J. Catal. 264 (2009) 67] of a stable oxygen species on non-porous Au/TiO_2 catalysts (TiO_2: P25, Degussa), which is active for CO oxidation and which can be reversibly deposited and removed by exposure to O_2 and CO pulses, respectively, we here present results of a TAP (temporal analysis of products) reactor study on the oxygen storage capacity ('OSC') for three Au/TiO_2 catalysts supported on mesoporous TiO_2 with different structural characteristics and its relation to the CO oxidation activity. The results are compared with the corresponding behavior of the non-porous Au/P25 supported catalyst. While the general reaction behavior of all catalysts is similar, there are distinct differences both in the absolute oxygen storage capacity and in its relation to the catalytic activity, depending on the nature of the support. The differences are associated with variations in the structure of the Au/TiO_2 interface and its perimeter, which is proposed as the adsorption site for active oxygen storage.

1. Introduction

Oxide supported Au catalysts have attracted considerable interest because of their high activity for various oxidation and reduction reactions at low temperatures [1–3], most prominently the CO oxidation reaction [4–7]. Despite extensive efforts to unravel the reaction mechanism and the physical origin of their high activity on a molecular scale (for reviews see [8,9]), however, essential features of the reaction such as (i) the nature of the active site, (ii) the activation of oxygen and the nature of the active oxygen species, (iii) the effect of the Au particle size on the catalyst activity, and (iv) the role of the support and metal-support interactions in the reaction and their influence on the catalytic activity are not yet resolved and are still under debate.

In recent quantitative measurements in a temporal analysis of products (TAP) reactor, we had demonstrated that oxide supported Au catalysts can reversibly store and reactively release 'active oxygen' upon exposure to O_2 pulses and upon subsequent reaction with CO pulses, respectively [10,11]. Hence, the existence of an active oxygen species, which is stable adsorbed on the catalyst surface at the reaction temperature, was directly demonstrated for the first time. This was shown first for Au/CeO_2 catalysts [10], and very recently also for Au/TiO_2 catalysts, which were supported on a commercial, non-porous TiO_2 material (P25, Degussa) [11]. For Au/TiO_2 catalyst with varying Au nanoparticle size, but with a similar Au loading, we could furthermore show that the amount of reversibly deposited 'active oxygen', the oxygen storage capacity (OSC), and the reactivity of the Au/TiO_2 catalysts scale about linearly with the perimeter of the interface between Au nanoparticles and TiO_2 support, providing strong support for a mechanism where oxygen activation and its reaction with CO occur at these perimeter sites [11]. This had been repeatedly postulated so far [5,12–16], however, hard experimental evidence was missing.

Recently, mesoporous oxides were introduced as alternative support materials, which may be attractive, e.g., because of their high surface area or the stabilization of the Au nanoparticles in the mesopores of the support [17–26]. In previous studies, we investigated the CO oxidation reaction and the deactivation behavior of mesoporous Au/TiO_2 catalysts with higher surface areas and comparable Au nanoparticle sizes, which were prepared via sol–gel processing in the presence of surfactants and subsequent Au loading by deposition–precipitation [22,26,27]. We could demonstrate that these catalysts surpass conventional Au/TiO_2 catalysts, which are based on commercial, non-porous TiO_2 material (P25, Degussa), in their activity for CO oxidation.

In the present publication, we report results of a TAP study on the ability of these catalysts to store active oxygen. We are particularly interested in the influence of the higher surface area of the support and its different modifications (pure anatase or rutile) on the OSC of the respective catalysts and its relation with their CO oxidation activity. For comparison, a standard Au/TiO_2 catalyst based on a commercial, non-porous TiO_2 material (P25, Degussa, mixture of 75% anatase and 25% rutile) was investigated as well.

* Corresponding author. Fax: +49 731 50 25452.
E-mail address: juergen.behm@uni-ulm.de (R.J. Behm).

0021-9517/$ - see front matter © 2009 Elsevier Inc. All rights reserved.
doi:10.1016/j.jcat.2009.06.020

The structural properties and the CO oxidation behavior (activity and deactivation) of these catalysts were described recently [26]. Using a highly stable and reproducible TAP reactor system [28], we first investigated the formation and reactive removal of active oxygen and quantified their amount on the differently supported Au/TiO_2 catalysts in multi-pulse TAP measurements, by alternating sequences of CO and O_2 pulses, respectively (Section 3.1). Subsequently, we evaluated the activity for CO oxidation on the different catalysts after oxidative pre-treatment (Section 3.2.1) and after defined changes of the surface oxidation state by sequences of simultaneous CO and O_2 pulses ('single-pulse measurements', Section 3.2.2), respectively. For the latter experiments, the surface state was changed in a controlled way by CO pulsing or by O_2 pulsing prior to the reaction. These experiments were also used to determine the amount of active oxygen present on the surface in steady-state under present reaction conditions ($CO:O_2 = 1:1$, 80 °C reaction temperature). Finally, the consequences of these results for the mechanistic understanding of the CO oxidation reaction on these Au/TiO_2 catalysts and of the effect of the mesoporous supports are discussed.

2. Experimental set-up and procedures

2.1. Preparation and characterization of the mesoporous support materials and the Au/TiO$_2$ catalysts

The preparation of the mesoporous support materials and the Au/TiO_2 catalysts was described in detail previously [26]. The mesoporous TiO_2 support material was prepared using an ethylene glycol-modified titanium precursor (bis(2-hydroxyethyl)titanate, EGMT) and a structure-directing surfactant to adjust the pore size and surface area of the resulting TiO_2 material [27]. For the mesoporous support denoted as "Brij", polyethyleneoxide hexadecylether (Brij56) was used as a structure-arranging surfactant. The second and third mesoporous supports denoted as 'SDS-A' and 'SDS-R' were synthesized using also EGMT as titania source, but using sodium dodecyl sulfate (SDS) as a surfactant. This results in a mesoporous material with a different surface area and pore diameter (see Table 1). Using different pH values during the synthesis with SDS as a surfactant resulted in different modifications for the materials 'SDS-R' (rutile) and 'SDS-A' (anatase). For comparison, we included a standard catalyst based on commercial P25 (Degussa) with a surface area of 56 $m^2\,g^{-1}$, consisting of a mixture of anatase and rutile. Further details on the preparation and on the post-treatment of the support materials, in order to remove the surfactant completely, can be found in Refs. [26,27].

Table 1
Structural and chemical properties of different mesoporous Au/TiO_2 catalysts and the standard Au/P25 catalyst after calcination in 10% O_2/N_2 for 30 min at 400 °C [26].

	Au/P25	Au/Brij	Au/SDS-A	Au/SDS-R
Au diameter (nm)[a]	3.0 ± 0.9	3.7 ± 0.9	3.0 ± 0.7	6.1 ± 1.5
Au loading (wt.%)[b]	2.6	2.6	2.6	4.8
TiO_2 modification[c]	75% anatase/25% rutile	Anatase	Anatase	Rutile
Pore volume in the mesoporous TiO_2	–	0.18	0.28	0.22
Pore size in the mesoporous TiO_2	–	7.5–8.2	4.4–6.3	[e]
Catalyst surface area ($m^2 g_{cat}^{-1}$)[d]	56	106	175	160
Dilution Au/TiO_2:SiO_2	1:1	1:1, 1:3	1:1	1:1, 1:3

[a] Determined by TEM.
[b] Determined by ICP-AES.
[c] Determined by XRD.
[d] Determined by low temperature N_2 adsorption (BET).
[e] Not well defined.

The Au/TiO_2 catalysts were prepared via a deposition–precipitation method, which had already been described in detail in Refs. [29,30], using the TiO_2 materials described above or non-porous TiO_2 (P25) as a support. Based on the surfactant used for the preparation of the support (SDS-R, SDS-A, Brij56) or on the name of the commercial support (P25), the resulting catalysts are denoted as Au/SDS-R, Au/SDS-A, Au/Brij, and Au/P25. To exclude subsequent modifications of the catalysts with time, the as-prepared samples were stored in the dark at low temperatures [31]. Prior to their use in TAP reactor measurements, the samples were dried at 100 °C in a flow of Ar for 15 h [32] (see also Ref. [26]) and were subsequently pre-treated by *in-situ* calcination in 10% O_2/N_2 at a flow rate of 20 Nml min^{-1} at 400 °C for 30 min [33], resulting in well-defined, fully oxidized catalysts as the starting point for subsequent pulse measurements.

The structural properties and the catalytic activity for CO oxidation of the resulting catalysts were determined previously by transmission electron microscopy (TEM), X-ray photoelectron spectroscopy (XPS), X-ray diffraction (XRD), N_2 adsorption (BET measurements) and by micro-reactor measurements at atmospheric pressure under differential reaction conditions [26]. The resulting characteristics are summarized in Tables 1 and 2, respectively. Specially, the different surface areas and modifications of the support materials should be noted, which were determined by the respective preparation procedure. When Brij56 was used as a structure-arranging surfactant, the corresponding catalyst (Au/Brij) had a surface area of 106 $m^2\,g^{-1}$ and an average pore size of 7.5–8.2 nm. The Au/SDS-A and Au/SDS-R catalysts had higher surface areas (175 $m^2\,g^{-1}$ and 160 $m^2\,g^{-1}$, respectively) and lower pore diameters (4.4- 6.3 nm, Au/SDS-A) or pores that were not well defined (Au/SDS-R), respectively. The non-porous Au/P25 catalyst finally had a surface area of 56 $m^2\,g^{-1}$. Moreover, the mesoporous supports consisted either of pure anatase (Au/SDS-A and Au/Brij) or pure rutile (Au/SDS-R), while P25 was a mixture of 75% anatase and 25% rutile. The gold content, measured by ICP-AES, was the same for Au/SDS-A, Au/Brij, and Au/P25 (2.6 wt.%) and was about

Table 2
CO oxidation activity and oxygen storage capacity (OSC) of different mesoporous Au/TiO_2 catalysts and of the standard Au/P25 catalyst after calcination in 10% O_2/N_2 for 30 min at 400 °C (TAP values for 1:3 diluted Au/Brij and Au/SDS-R catalysts).

	Au/P25	Au/Brij	Au/SDS-A	Au/SDS-R
Initial/steady-state activity for CO oxidation (atmospheric pressure)/10^{-4} mol $g_{Au}^{-1}\,s^{-1}$ [26]	34.3 9.4	87.1 25.7	37.2 12.4	34.8 9.2
Initial/steady-state activity for CO oxidation (atmospheric pressure)/10^{-4} mol $g_{cat}^{-1}\,s^{-1}$ [26]	0.89 0.24	2.26 0.67	0.97 0.32	1.67 0.44
Initial/steady-state turnover frequency for CO oxidation (atmospheric pressure)/s^{-1} [26]	2.0 0.5	6.3 1.9	2.2 0.7	4.2 1.1
Initial/steady-state turnover frequency for CO oxidation per Au perimeter site (atmospheric pressure)/s^{-1} [26]	12.2 3.1	46.5 14.0	13.5 4.3	49.3 12.9
TAP: CO conversion (%) under steady-state conditions	88	15	76	20
TAP: CO conversion (molecules CO) under steady-state conditions per pulse and perimeter site/10^{-2}	7.8	1.8	5.4	3.4
TAP: OSC (molecules $O_2 g_{cat}^{-1}$)	2.1×10^{18}	0.3×10^{18}	0.6×10^{18}	0.9×10^{18}
TAP: OSC (O atoms/perimeter site Au–TiO_2)	0.81	0.18	0.23	0.73

a factor of 2 higher for the Au/SDS-R catalyst (4.8 wt.%). Also the average diameters of the Au nanoparticles after calcination were rather similar for Au/SDS-A, Au/Brij, and Au/P25 (3.0 nm for the Au/P25 and the Au/SDS-A catalysts and 3.7 nm for the Au/Brij catalyst) and again higher for the Au/SDS-R catalyst (6.1 nm). XPS measurements of the catalysts performed after conditioning showed that Au mainly existed in its metallic Au^0 state with a Au(4f) binding energy of 84.0 ± 0.1 eV [34,35].

2.2. TAP reactor measurements

The pulse experiments were carried out in a home-built TAP reactor [28], which is largely based on the TAP-2 approach of Gleaves et al. [36]. In short, piezo-electric pulse valves were used to generate gas pulses of typically about 8×10^{15} molecules per pulse. For all the measurements presented, these pulses contained 50% Ar as an internal standard to enable quantitative evaluation on an absolute scale. The gas pulses were directed into a quartz tube micro-reactor. The catalyst bed was located in its central part and was fixed by two stainless steel sieves (Haver & Boecker OHG, transmission 25%). Ten milligrams of the catalyst were diluted with SiO_2 ('gebaflot 010' from Dorfner GmbH, grain size 100–200 μm) in a ratio of 1:1 (Au/P25, Au/Brij, Au/SDS-A, and Au/SDS-R) or 1:3 (Au/Brij, Au/SDS-R). This resulted in comparable pulse durations over the 1:1 Au/SDS and Au/P25 samples, while on the Au/Brij (1:1) and Au/SDS-R (1:1) samples the pulses were about double as long as on the other catalysts. Therefore, we also used more strongly diluted Au/Brij (1:3) and Au/SDS-R (1:3) samples (with the same amount of active catalyst) in an additional series of experiments. The diluted catalysts were packed between two layers of SiO_2, resulting in a three-zone catalyst bed [37] with a total mass of 150 mg for all samples (10 mg of the pure catalyst and 140 mg of SiO_2) and a total catalyst bed length of about 8 mm. The metal sieves and the SiO_2 were checked earlier to be catalytically inactive in the temperature range investigated [10]. After passing through the catalyst bed and a differentially pumped gate valve, the gases propagated into the analysis chamber where they were analyzed by a quadrupole mass spectrometer (Pfeiffer Vacuum, QMG 700). The analysis chamber was pumped by two turbomolecular pumps (Pfeiffer Vacuum, TPU 2101P and 1001P), resulting in a base pressure of less than 2×10^{-9} mbar during the measurements. The home-built differentially pumped gate valve [28] allows to (i) connect the end of the reactor tube directly to the analysis chamber, (ii) close the reactor and analysis chamber to allow for sample exchange, or (iii) close only the analysis chamber and open a connection from the reactor to a roughing pump. In the latter case, the reactor can be operated under continuous flow conditions at atmospheric pressure. This mode is used, e.g., for *in-situ* catalyst conditioning (with reduced pumping speed) or for evacuating the reactor before opening the connection to the analysis chamber [28]. All measurements were performed at 80 °C reaction temperature.

3. Results and discussion

Within this study, two types of TAP measurements were performed, either admitting sequences of CO/Ar or O_2/Ar pulses, respectively, to the catalyst in order to deposit or reactively remove active oxygen from the catalyst surface and thus change its oxidation state (multi-pulse experiments), or simultaneously admitting CO/Ar and O_2/Ar pulses to evaluate the activity for CO oxidation ($CO:O_2 \approx 1:1$). During the simultaneous pulse sequences the amount of active oxygen on the surface may change as well, which can be derived by comparing the stoichiometry of CO and O_2 consumption for CO_2 formation. Furthermore, in both types of measurements the formation of stable, adsorbed carbon-containing species can, at least in principle (see below), be determined from the carbon balance by comparison of the CO consumption and CO_2 desorption. Based on the results of previous *in-situ* IR spectroscopic measurements, which showed a rapid build-up of surface carbonate species during the reaction [26], and since CO_2 adsorption is weak on these catalysts, deficits in the carbon balance would be attributed to the formation of stable, adsorbed surface carbonates.

3.1. Multi-pulse TAP reactor measurements

Following the previous study on Au/P25 [11], we first tested whether active oxygen species, which are reactive for the CO oxidation and which are stable on the surface of a mesoporous Au/

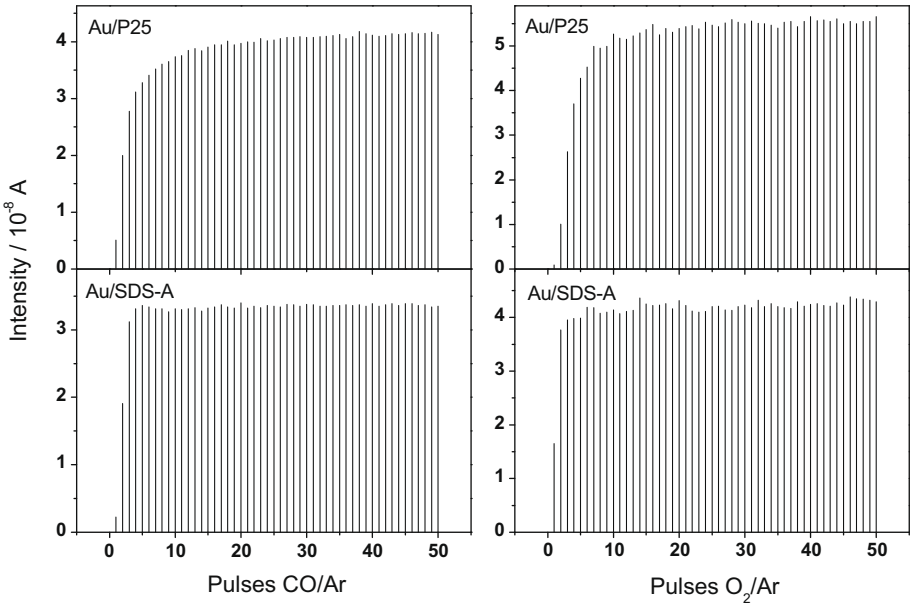

Fig. 1. Pulse responses during a multi-pulse experiment performed at 80 °C over the Au/P25 and the Au/SDS-A catalysts after calcination in 10% O_2/N_2 for 30 min at 400 °C.

TiO_2 catalyst at a typical reaction temperature of 80 °C, can be formed upon calcination or O_2 pulsing. The time between single pulses for these multi-pulse experiments was chosen to be 10 s, which was large enough for the educt gases to completely pass through the catalyst bed before the next pulse was admitted. Considering the rather low temperature and the duration of the pulse sequences (16 min for the O_2 pulse sequence and 33 min for CO), oxygen storage can be assumed to be an essentially pure surface reaction, rather than being dominated by bulk diffusion processes.

In these measurements, we alternately exposed the catalysts to sequences of 200 CO/Ar and 100 O_2/Ar pulses, which were found to be sufficient to reach stable catalyst conditions. At the end of the respective sequences, we could not detect any consumption of the reactive gases. This is illustrated in representative sequences of pulse responses obtained on the Au/P25 and the Au/SDS-A catalysts, respectively, in Fig. 1. It is already clear from the raw data that the OSC of the Au/SDS-A catalyst was significantly lower than that of the Au/P25 catalyst. A detailed discussion on the quantitative differences for all catalysts is given below.

The amount of CO or O_2 consumed during these experiments, when exposing the oxidized catalyst to CO pulses or the reduced catalyst to O_2 pulses, respectively, is shown in Fig. 2 for the Au/P25 catalyst. The consumption within one pulse sequence, calculated from the missing amount of reactant gas within each single pulse, was highest at the beginning and got smaller with increasing saturation of the catalyst surface, until there was no more uptake detectable. The general behavior was the same over all samples, only the total amounts of reactive gas consumption were different for each sample. As has been described already in Ref. [11], the first pulse sequence of CO directly after conditioning in O_2 showed a distinctly higher amount of CO consumption and CO_2 production compared to the following sequences. It was also significantly higher than the amount of active oxygen taken up in the following sequence of O_2 pulses, while in the later sequences the uptake and reactive release of active oxygen were identical. Hence, in the subsequent cycles active oxygen deposition and removal were fully reversible. The observation of a higher amount of active oxygen removal in the first sequence of CO pulses indicates that O_2 pulsing was not sufficient to completely fill all adsorption sites for active oxygen which were accessible during calcination in O_2 at 400 °C. Finally, the carbon mass balance also shows no measurable difference between CO consumption and CO_2 formation, indicating that the build-up of carbon containing species on the surface was below the detection limit of these measurements.

The absolute amounts of CO consumption and O_2 consumption determined for the different catalysts are illustrated in Fig. 3, which shows (i) the amount of CO consumed during the first sequence of CO pulses after O400 pre-treatment, (ii) the amount of CO consumed after the reversible storage of oxygen on the catalysts by O_2 pulses, and (iii) the absolute amount of oxygen that can be stored on the reduced surface, after CO pulsing, and subsequently reacted away by CO pulses (OSC). For better comparison, the amount of O_2 consumption is multiplied by a factor of two to account for the reaction stoichiometry. The corresponding values are also listed out in Table 2. For all four catalysts, the amount of active oxygen deposited during calcination was significantly higher than that reversibly deposited/removed during subsequent pulse sequences. The relative differences, however, varied significantly, ranging from a factor of 2.4 (Au/P25) to a factor of 7.6 (Au/Brij). Furthermore, the absolute amount of reversible active oxygen uptake also varied considerably between the catalysts, with significantly lower active oxygen uptake on the mesoporous Au/TiO_2 catalysts (0.9×10^{18}, 0.6×10^{18}, and 0.3×10^{18} molecules O_2 g_{cat}^{-1} for the Au/SDS-R, Au/SDS-A, and Au/Brij catalysts, respectively) than on the non-porous Au/P25 catalyst (2.1×10^{18} molecules O_2 g_{cat}^{-1}).

Obviously, there is no correlation between the OSC and the surface area of the support for the different mesoporous and non-porous catalysts investigated. In this respect, it is important to note that for all catalysts the total amount of active oxygen removable from the surface is only a very small fraction of the total surface oxygen (0.74% for Au/P25, 0.07% for Au/SDS-A, 0.11% for Au/SDS-R, and 0.06% for the Au/Brij catalysts). The OSC was highest on

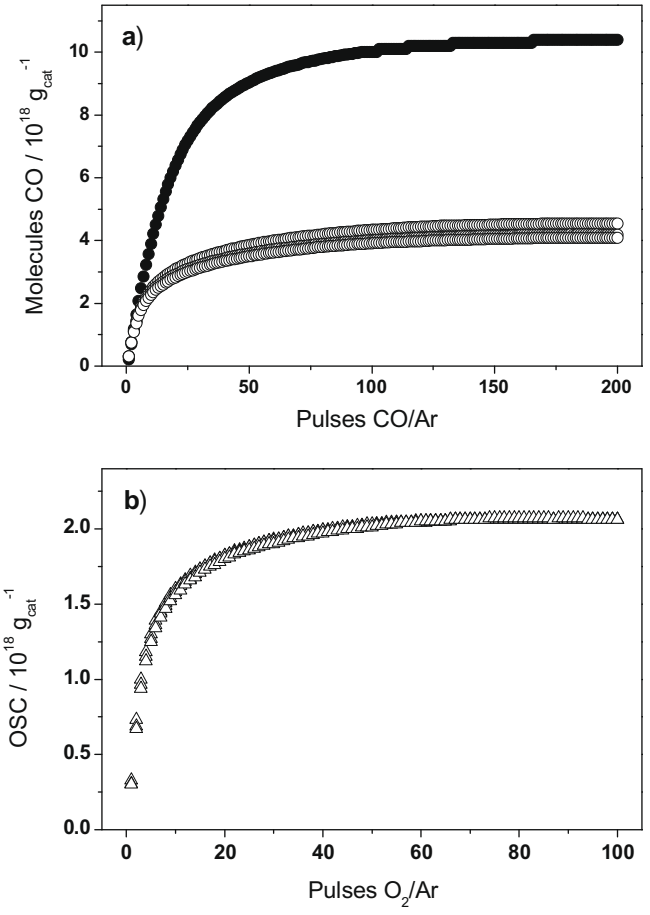

Fig. 2. Total amount of (a) CO and (b) O_2 consumed during the multi-pulse experiments at 80 °C on the Au/P25 catalyst after calcination in 10% O_2/N_2 for 30 min at 400 °C (O400) during three oxidation/reduction cycles. The filled symbols in (a) represent the CO consumption during the first sequence after calcination.

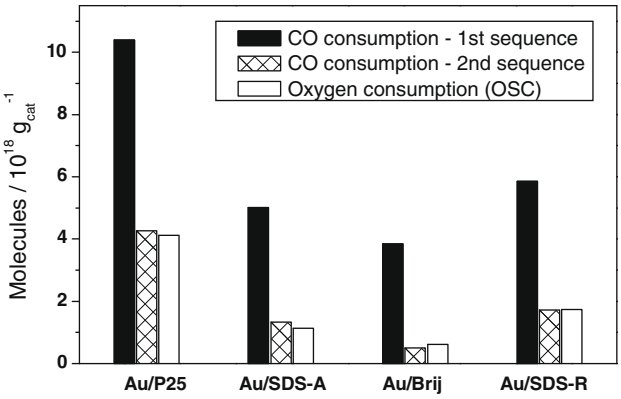

Fig. 3. Comparison of the (reversible) OSC (oxygen atoms) and the amount of CO consumed during the multi-pulse experiments at 80 °C over the differently supported catalysts after calcination in 10% O_2/N_2 for 30 min at 400 °C (O400).

the Au/P25 sample, which had the lowest surface area, and was significantly lower on the mesoporous catalysts, whose surface areas were between twofold and threefold as high. This result is consistent with our previous conclusion for Au/P25 that the surface area is not the dominant factor determining the OSC (see below) [11]. It should also be noted that the mesoporous catalysts consisted either only of (defect rich) anatase or only of rutile, while P25 consisted of a mixture of anatase and rutile.

In our previous study on similar type Au/P25 catalysts with identical Au loading but with different particle sizes, we had found that the OSC scales about linearly with the number of perimeter sites at the interface between Au nanoparticles and TiO_2 support [11]. Assuming hemispherical Au particles for all catalysts and using the mean Au particle sizes and Au loadings of the different catalysts (see Table 1), we can calculate the local coverage of active oxygen species per perimeter Au atom (this is calculated for adsorbed oxygen atoms, for details see [11]). This results in local oxygen coverages of 0.81 (Au/P25), 0.73 (Au/SDS-R), 0.23 (Au/SDS-A), and 0.18 (Au/Brij).

The present results demonstrate that the Au–TiO_2 interface perimeter length is not the only factor determining the OSC. Apparently, the situation is more complex when comparing Au/TiO_2 catalysts supported on different TiO_2 materials than for catalysts based on the same support material. Most simply, the different OSCs of the mesoporous and non-porous Au/TiO_2 catalysts can be understood by assuming that the structure and chemical nature of the Au–TiO_2 interface perimeter differ for the different TiO_2 materials, with fewer accessible adsorption sites for active oxygen on the mesoporous catalysts, in particular on the anatase-based catalysts, than on the non-porous standard Au/P25 catalyst. However, other, more complex effects cannot be ruled out, e.g., carbon impurities resulting from the synthesis of the mesoporous materials. Such residues were in fact detected by DRIFTS measurements on the mesoporous catalyst after the same conditioning as used here, but not on Au/P25 [26]. Also the modification of the support may play an important role.

Finally, the direct correlation between OSC and the CO oxidation activity, which was observed for Au/P25 catalysts with different Au particle sizes [11], also did not exist when comparing the Au/TiO_2 catalysts supported on different TiO_2 materials. The OSC on the Au/SDS-A catalyst was by a factor of about 4 lower than that on the Au/P25 catalyst, although the CO oxidation activity in TAP reactor measurements (description see below) was only slightly lower compared to Au/P25. This will be discussed in more detail in the following section, after presenting the single-pulse measurements.

3.2. Simultaneous pulse TAP reactor measurements

The activity for CO oxidation at 80 °C was evaluated during simultaneous pulses of CO/Ar and O_2/Ar, both from the consumption of O_2 and CO and from the formation of CO_2 which were detected at the reactor exit. In these TAP measurements, the time between subsequent pulses was 40 s, in order to reach the base line again for all educt (CO, O_2) and product (CO_2) gases before the next pulse was admitted.

To allow for a meaningful quantitative comparison of the catalytic performance of the different catalysts, the pulse duration and hence the residence time of the educts within the catalyst bed should be identical. Using the same dilution for all four catalysts (Au/TiO_2:SiO_2 = 1:1) resulted in comparable pulse durations for Au/P25 and Au/SDS-A, while the residence time was much higher for the Au/Brij and the Au/SDS-R catalysts (not shown). Since there was essentially no interaction between the inert Ar and the catalyst surface, the longer residence time compared to the Au/P25 and Au/SDS-A catalysts must be due to slower diffusion processes in these catalysts. To decrease the residence time for the Au/Brij and the Au/SDS-R catalysts, their dilution was changed from 1:1 to 1:3, resulting in a less densely packed catalyst zone and hence faster diffusion of the incoming gas pulses through the catalyst bed. As can be seen in Fig. 4, the residence time of Ar was the same for all catalysts when using the more highly diluted Au/Brij and Au/SDS-R catalysts. It should be noted that the SiO_2 particles are very large (average grain size 100–200 μm) compared to the TiO_2 particles (21 nm for P25, agglomerates of even smaller particles for the mesoporous TiO_2 materials). To keep the mass of the pure catalyst constant, the amount of SiO_2 before and after the catalyst zone in the three zone catalyst bed was decreased accordingly.

3.2.1. CO oxidation after oxidative conditioning

Simultaneous pulse reaction measurements, performed directly after catalyst calcination and evacuation of the reactor, are illustrated in Fig. 5. The general behavior was the same over all four catalysts, showing a decreasing CO consumption/CO_2 formation and an increasing O_2 consumption, until a steady-state situation was reached. At that point, the consumption of CO and O_2 and the formation of CO_2 were essentially stoichiometric. The initial difference in CO and oxygen consumption reflects a reactive removal of active oxygen from the catalyst surface by CO, equivalent to a reduction of the catalyst surface. Hence, part of the oxygen present on the surface after calcination was removed by reaction with CO, although the reaction atmosphere created by the approximately similar pulse intensities of the CO/Ar and O_2/Ar pulses contained a 2:1 excess of O_2. From the carbon balance, with essentially similar CO consumption and CO_2 formation, we concluded that after *in-situ* calcination the build-up of adsorbed carbon-containing species was below the detection limit of the measurements. This is in contrast with our previous findings on an *ex-situ* calcined Au/P25 catalyst, where a measurable deficit in the carbon balance pointed to the build-up of such species during the CO/O_2 pulses [11].

The evolution of the CO conversion with ongoing pulse number exhibits characteristic differences between the different catalysts. For all catalysts, the CO conversion was highest at the beginning of the pulse sequence, reaching almost complete conversion (100% conversion). For information, complete CO consumption is indicated by dashed lines in Fig. 5. With increasing pulse number, the CO conversion decreased. This decrease was rather subtle for the Au/P25 catalyst, slightly more pronounced for the Au/SDS-A catalyst, and rather dramatic for the Au/Brij and the Au/SDS-R catalysts. Both for the 1:1 diluted and the 1:3 diluted Au/Brij catalysts, the CO conversion decreased rapidly, reaching 50% and 16% of the

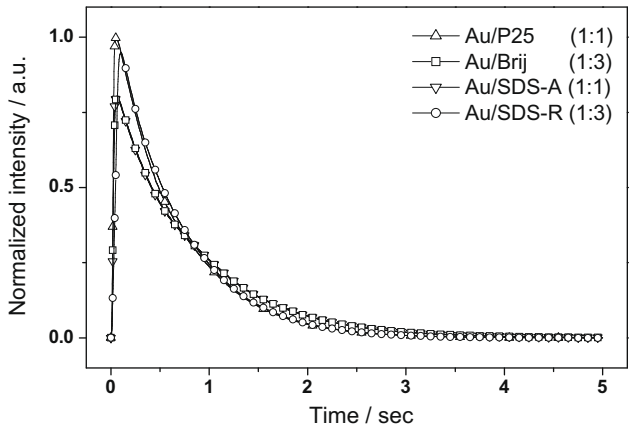

Fig. 4. Pulse shapes of the area-normalized signals of Ar on the different O400 pretreated Au/TiO_2 catalysts used for the simultaneous pulse experiments at 80 °C.

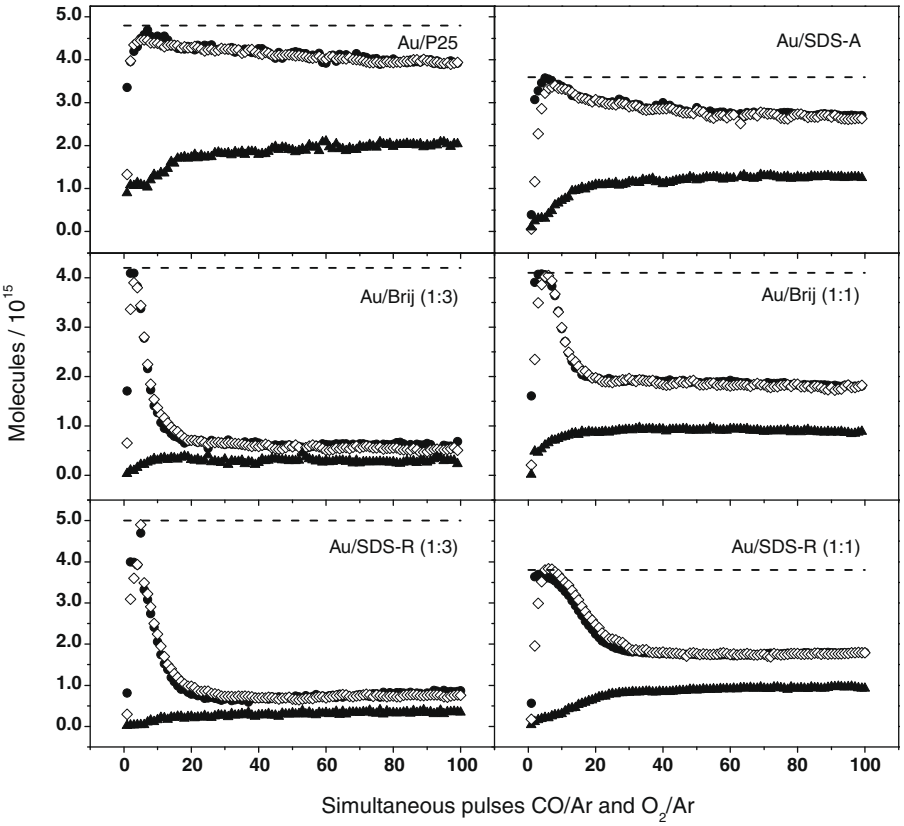

Fig. 5. CO uptake (•), O_2 uptake (▲), and CO_2 formation (◇) during simultaneous CO/Ar and O_2/Ar pulses at 80 °C on the Au/TiO_2 catalyst after calcination in 10% O_2/N_2 for 30 min at 400 °C (O400). The dashed lines indicate the number of consumed CO/produced CO_2 molecules for complete conversion of the CO pulses admitted to the micro-reactor.

initial maximum value after 30 pulses, and qualitatively the same was true for the Au/SDS-R catalysts. For further increasing pulse number, the CO oxidation activity remained essentially constant, except for the Au/P25 catalyst, where it continued to decay slightly (∼3%). After 100 pulses, steady-state conditions were reached for all catalysts. At that point, the CO conversions were 91% (Au/P25), 76% (Au/SDS-A), 20% (Au/SDS-R (1:3)), and 15% (Au/Brij (1:3)), respectively. The high initial activities can be explained by the presence of larger amounts of active oxygen on the catalysts after calcination. The less pronounced decrease in activity for the less diluted Au/Brij (1:1) (final conversion 50%) and Au/SDS-R (1:1) catalysts (final conversion 47%) compared to the more strongly diluted Au/Brij (1:3) and Au/SDS-R (1:3) catalysts is tentatively explained by the longer residence time of the reactants in the catalyst zone on the less diluted catalysts, illustrating the influence of diffusion processes within the catalyst bed on the catalytic activity measured in the TAP experiment. (Note that the total amount of the catalysts was the same in both cases.)

The observation of about similar CO oxidation activities on the Au/P25 and the mesoporous Au/SDS-A catalysts and of much lower steady-state CO conversions on the Au/Brij and Au/SDS-R catalysts in the TAP reactor measurements can be compared with kinetic results obtained in micro-reactor measurements at atmospheric pressure. In order to obtain differential reaction conditions, with CO conversion <20%, the catalysts were highly diluted in these measurements. For the same catalysts investigated in the present study, Denkwitz et al. measured reaction rates on the freshly calcined catalyst and their variation over 1000 min on stream for all catalysts (1% CO, 1% O_2, rest N_2, atmospheric pressure, 80 °C reaction temperature) [26]. The resulting initial and final rates are listed out in Table 2 as mass-normalized rates (Au mass and catalyst mass) and as TOF numbers. Comparing the results of the TAP conversion measurements and of the kinetic measurements (catalyst mass-normalized activities), we found that the order of the catalytic activity for the CO oxidation was completely reversed in these two cases. The TAP conversion decreased in the order Au/P25 > Au/SDS-A > Au/SDS-R > Au/Brij, while for the kinetic measurements the order was opposite. These differences did not disappear when using TOF numbers, or TOF numbers normalized to the number of Au perimeter sites (see Table 2). The differences between the two types of activity measurements are most likely related to the differences in the diffusion properties of the different catalysts due to the higher surface area and the pore structure of the mesoporous supports. This was especially true for the Au/Brij and the Au/SDS-R catalysts, which showed a higher residence time for the inert Ar standard in the TAP reactor measurements when using the same dilution as for the Au/P25 and Au/SDS-A catalysts (1:1 dilution) (see Fig. 4). This required the use of higher dilutions for the Au/Brij and the Au/SDS-R catalysts (1:3 dilution) in TAP reactor measurements in order to obtain the same residence time for all catalysts. In the mixed catalyst bed, consisting of Au catalyst and SiO_2, part of the reactant molecules may not or less often reach the active centers within the pores of the support and instead pass through channels provided by the SiO_2 particles in direction of the reactor exit. This would result in a lower CO conversion in the TAP measurements compared to the other two catalysts as it is observed experimentally. This tentative explanation is supported by the higher steady-state CO conversion during simultaneous pulse TAP reactor measurements when using less diluted (1:1 dilution) Au/Brij and Au/SDS-R catalysts. Effects of the pore diffusion on the CO oxidation activity of the different Au catalysts will be investigated in more detail in a forthcoming study.

Furthermore, the OSC and the CO oxidation activity also did not follow the same order, neither the TAP conversion-based activities nor the steady-state activities in the kinetic measurements. This discrepancy differs distinctly from our previous observations of an almost linear correlation between the turnover frequency in atmospheric pressure measurements and the OSC, which was obtained in TAP reactor measurements for Au/P25 catalysts with identical Au loading, but with different Au particle sizes [11]. Obviously, the close correlation between OSC and CO oxidation activity is valid only for similar type catalysts.

Finally, we used the data shown in Fig. 5 to determine the amount of active oxygen present on the catalyst under steady-state reaction conditions. From the quantitative evaluation of the CO_2 formation/CO consumption and of the O_2 consumption, we calculated the amount of active oxygen, which was reactively removed from the calcined catalyst during the CO oxidation reaction under present reaction conditions until reaching steady-state conditions. The corresponding amounts of the additionally converted oxygen atoms from the catalyst after the O400 treatment were 5.3×10^{18} O atoms g_{cat}^{-1} for Au/P25, 4.5×10^{18} O atoms g_{cat}^{-1} for Au/SDS-A, 4.0×10^{18} O atoms g_{cat}^{-1} for Au/SDS-R, and 2.6×10^{18} O atoms g_{cat}^{-1} for Au/Brij (see Table 3). These results can be compared with the loss of active oxygen determined for initial reduction (CO pulsing) and subsequent re-oxidation (O_2 pulsing) of the calcined catalysts, which was determined in the multi-pulse experiments. This sequence also results in the oxidized state of the catalyst (see Section 3.1). The resulting values are listed out in Table 3. They indicate that, within the precision of the measurements of $\pm 0.1 \times 10^{15}$ molecules per pulse ($\pm 0.3 \times 10^{18}$ molecules O_2 g_{cat}^{-1}), the catalyst surface composition during CO oxidation in simultaneous TAP pulses (steady-state, present reaction conditions) is close to that of the 'oxidized state' obtained after O_2 pulsing.

3.2.2. CO oxidation after defined changes of the catalyst surface

For more direct conclusions on the state of the catalyst during the CO oxidation reaction in simultaneous TAP pulses, this question was investigated in more detail by using catalysts which were pre-treated such that the reaction started directly with a reduced or oxidized catalyst, respectively. This was done by similar single-pulse measurements as described in the previous section by using catalysts which were first exposed to the reaction mixture to reach steady-state conditions and were subsequently either oxidized by a subsequent sequence of 100 pulses O_2/Ar or reduced by a subsequent sequence of 200 pulses CO/Ar. The resulting catalysts are described as 'oxidized' or 'reduced', where these states refer to oxidation or reduction to the extent possible by O_2 pulsing or CO pulsing.

On the Au/P25 catalyst, exposure of the steady-state catalyst to the O_2 pulses caused only little oxygen uptake, about 3.0×10^{17} molecules O_2 g_{cat}^{-1} (not shown). Subsequent CO oxidation after this oxidative pre-treatment showed an essentially constant consumption of CO during the 100 pulse sequence and an essentially stoichiometric consumption of O_2 within the accuracy of these measurements (Fig. 6). The latter is illustrated graphically by the close agreement between consumption of CO and oxygen in Fig. 6 when using the number of O atoms. Both these results indicate that the steady-state of the catalyst surface during CO oxidation in a 2:1 excess of O_2 in the reaction atmosphere is very close to the 'oxidized' state obtained after O_2 pulsing. Comparable results were also obtained over the mesoporous Au/TiO_2 catalysts, pointing to a similar surface state also on these catalysts during CO oxidation. Similar to that shown in Fig. 5, CO_2 formation is essentially identical to CO consumption and therefore not shown. Hence, within the precision of the measurement all CO consumed was converted to CO_2.

This conclusion is also supported by similar activity measurements performed on 'reduced' catalysts which after the reaction were exposed to 200 CO pulses. As illustrated in Fig. 7 for the four catalysts, the O_2 consumption over all samples was higher during the first 40 simultaneous pulses CO/Ar and O_2/Ar compared to the consumption of CO and the formation of CO_2, which as shown in Figs. 5 and 6 is essentially identical to the CO consumption and therefore not shown. Hence, during the reaction the pre-reduced catalysts were re-oxidized again. After that period, a steady-state was reached, which was characterized by stoichiometric consumption of O_2 and CO, which is illustrated by the complete agreement between consumption of CO and O atoms in Fig. 7, and the catalyst surface is again close to its 'oxidized' state.

For the Au/P25 catalyst, the amount of additionally consumed O_2 during this period was 1.7×10^{18} molecules O_2 g_{cat}^{-1}. This is almost identical to the amount of oxygen reactively removed from the surface by the sequence of 200 CO/Ar pulses (see above) after the CO oxidation reaction (3.3×10^{18} surface oxygen atoms g_{cat}^{-1}) for the Au/P25 catalyst, and also close to the measured OSC of 2.1×10^{18} molecules O_2 g_{cat}^{-1}. These results clearly demonstrate that for the Au/P25 catalyst (i) the steady-state composition of the catalyst surface during reaction in 2:1 O_2 excess is close to that obtained after O_2 pulsing, and (ii) this state does not depend on the history of the catalyst. Starting with an O_2-pulsed 'oxidized' catalyst resulted in the same steady-state catalyst surface as starting with a CO-pulsed 'reduced' catalyst. Furthermore, within the

Table 3
Loss of active oxygen of the different Au/TiO_2 catalysts in the oxidized and reduced state (multi-pulse experiments), respectively, and under steady-state reaction conditions (simultaneous CO/O_2 pulsing), always relative to the freshly calcined catalyst (calcination in 10% O_2/N_2 for 30 min at 400 °C, 1:3 diluted Au/Brij and Au/SDS-R catalysts).

State of the catalyst	Au/P25	Au/Brij	Au/SDS-A	Au/SDS-R
Loss of active oxygen in the reduced state/O atoms g_{cat}^{-1}	10.4×10^{18}	3.9×10^{18}	5.0×10^{18}	5.9×10^{18}
Loss of active oxygen in the oxidized state/O atoms g_{cat}^{-1}	6.1×10^{18}	3.4×10^{18}	3.8×10^{18}	4.2×10^{18}
Loss of active oxygen during CO oxidation, under steady-state conditions/ O atoms g_{cat}^{-1}	5.3×10^{18}	2.6×10^{18}	4.5×10^{18}	4.0×10^{18}

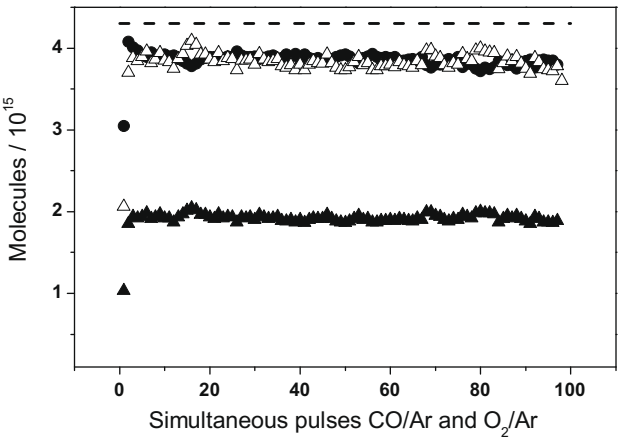

Fig. 6. CO uptake (•) and O_2 uptake (▲) during simultaneous CO/Ar and O_2/Ar pulses at 80 °C on the Au/P25 catalyst after reaching steady-state reaction conditions and subsequent oxidation by 100 pulses O_2/Ar. For better comparison between CO and oxygen consumption, the consumption of atomic oxygen is also plotted (△). The dashed line indicates the number of consumed CO molecules for complete conversion of the CO pulses admitted to the micro-reactor.

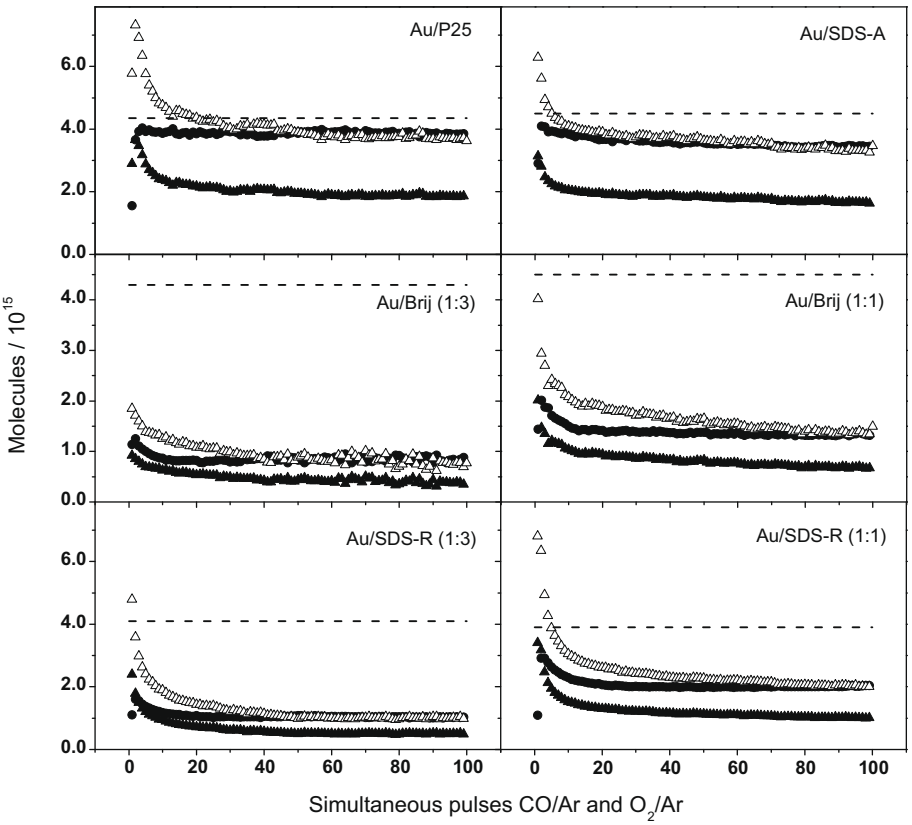

Fig. 7. CO uptake (•) and O_2 uptake (▲) during simultaneous CO/Ar and O_2/Ar pulses at 80 °C on the differently supported Au/TiO_2 catalysts after reaching steady-state reaction conditions and subsequent reduction by 200 pulses CO/Ar. For better comparison between CO and oxygen consumption, the consumption of atomic oxygen is also plotted (△). The dashed lines indicate the number of consumed CO molecules for complete conversion of the CO pulses admitted to the micro-reactor.

resolution of the measurements, we did not find a measurable change in CO_2 formation activity while re-oxidizing the catalyst.

For the mesoporous Au/TiO_2 catalysts, a similar quantitative evaluation was hardly possible due to the much lower activities and/or the lower OSC values, which also limit the amount of active oxygen removable per pulse. But it is clear that there is essentially no change in the oxidation state of the catalyst (no additional CO consumption) on the 'oxidized' surfaces obtained upon O_2 pulsing. In contrast, starting with the reduced catalyst obtained after CO pulsing, we found re-oxidation of the catalyst to occur, as evident from the higher oxygen consumption compared to the CO consumption during the first 30 simultaneous pulses. This clearly confirms our previous conclusion (see Section 3.2.1) that for all catalysts investigated and under present reaction conditions (simultaneous pulsing) the oxidation state during CO oxidation is close to the oxidized state obtained upon O_2 pulsing.

Surprisingly, for all catalysts, the conversion of CO during the activity measurements on the pre-reduced catalysts was lower only during the first one or two pulses, and then reached values slightly higher than those of the steady-state conversion, and finally decayed slowly to the steady-state activity, which was reached after about 40 pulses. For the Au/P25 and the Au/SDS-A catalysts, the initial CO conversion/CO_2 formation (not shown) were close to complete CO consumption, which was close to complete CO consumption indicated by the dashed lines. In contrast, for the 1:3 diluted Au/SDS-R and Au/Brij catalysts, the initial CO conversion/CO_2 formation (not shown) also were distinctly lower than the limit of complete CO conversion, which was at least partly due to the transport effects discussed before. On the less strongly diluted (1:1 dilution) Au/SDS-R and Au/Brij catalysts, the maximum CO consumption was significantly higher than that on the 1:3 diluted catalysts. It was close to complete CO consumption for the Au/SDS-R catalyst, and significantly below complete conversion for the Au/Brij catalyst. From these observations we conclude that the formation of the active oxygen species for CO oxidation is fast on all catalysts. The presence of a maximum in CO conversion after few pulses, which was observed on the mesoporous catalysts, indicates that the most active state of the surface, under present reaction conditions, is reached at an oxygen vacancy concentration which is slightly higher than that during CO oxidation under steady-state conditions. Similar observations were also reported recently for CO oxidation on Au/CeO_2 catalysts [10].

4. Summary and conclusions

Using a highly stable TAP reactor set-up, we have investigated the formation and reactive removal of stable adsorbed oxygen, which is reactive for the CO oxidation reaction on mesoporous and non-porous Au/TiO_2 catalysts with comparable Au loading and Au particle sizes by multi-pulse and single-pulse experiments. The experiments focused on the differences in oxygen storage capacity and CO oxidation activity when changing the nature of the support from conventional, non-porous P25 to mesoporous TiO_2. The main results of these measurements and the resulting conclusions are as follows:

1. On all catalysts, stable, adsorbed reactive oxygen is formed by calcination at 400 °C as well as by exposure to O_2 pulses at 80 °C. Calcination always results in a higher amount of active oxygen than exposure of a 'reduced' catalyst to a sequence of O_2 pulses at 80 °C. After the initial reduction cycle, re-deposition of active oxygen and its reactive removal by exposure to

sequences of O_2 and CO pulses, respectively, are fully reversible. The oxygen storage capacity of the mesoporous catalysts (reversible active oxygen per gram catalyst) is significantly lower than that of the non-porous Au/P25 catalyst, for the initial oxygen deposition both during calcination and during reversible pulsing.

2. Comparing the oxygen storage capacity of the different catalysts, this is neither correlated to the overall surface area of the catalysts, nor does it scale with the number of (accessible) perimeter sites at the interface between Au nanoparticles and TiO_2 support: The surface areas are significantly higher for the mesoporous catalysts than for the Au/P25 catalyst, while the OSC is highest on the latter catalyst, and the coverage of active oxygen relative to the interface perimeter sites varies between 0.18 (Au/Brij) and 0.81 (Au/P25). Hence, the OSC is little affected by the overall surface area of the catalysts, and the number of perimeter sites is not the only important parameter for determining the OSC. We propose that as an additional factor, the nature of the support also and hence the structure/chemical nature of the interface perimeter sites are decisive for the OSC. This includes different support modifications, as evidenced by the difference between Au/SDS-R and Au/SDS-A, as well as the modifications of the interface perimeter due to chemical effects such as carbon residues, which are possibly present at the interface of the mesoporous supports. For Au/TiO_2 catalysts supported on the same support material, as it was the case in our previous study on Au/P25 catalysts with different Au particle sizes, such effects play no role, and the number of perimeter sites is left as the main parameter. For catalysts supported on different materials, the latter effects can become equally important.
3. For all catalysts investigated, the oxidation state of the catalyst surface during reaction in simultaneous CO and O_2 pulses, in an excess of O_2 (identical pulse intensities for CO and O_2 result in a 2:1 oxygen excess), is close to the 'oxidized' state obtained upon O_2 pulsing on a reduced catalyst. The surface state of the catalysts and also the CO oxidation activity of the catalysts under steady-state conditions, during simultaneous CO/Ar and O_2/Ar pulses, are independent of the previous history of the catalyst (calcination, exposure to reaction atmosphere and subsequent reduction by CO pulses, exposure to reaction atmosphere and subsequent oxidation by O_2 pulses). Accordingly, reaction on the 'oxidized' catalysts results in stoichiometric consumption of CO and O_2, while for reaction on the 'reduced' catalysts obtained by CO pulsing, additional O_2 is consumed initially, during the first 40 pulses, which is used to re-oxidize the surface. Hence, also under reaction conditions, the build-up of reactive adsorbed oxygen is very fast.
4. For all catalysts, the apparent reactivity of the catalysts, as measured by the CO consumption, is lowest in the reduced state (first pulses in the sequences shown in Fig. 7), higher in the oxidized state, and highest after calcination or in a state with slightly less active oxygen than after calcination (Au/SDS-A). This is easily explained by the increasing presence of active oxygen present on the respective surfaces in this order.

In total, the variation of the support material has a distinct influence on the ability of the resulting Au/TiO_2 catalysts to store active oxygen, which can also be described as the redox behavior of the catalysts, and on their catalytic performance for CO oxidation. We propose that for the different mesoporous TiO_2 substrate investigated in this study also the interface perimeter sites act as active sites for the adsorption of active oxygen and for CO oxidation reaction, in agreement with our recent prediction for Au/P25 [11], but that the adsorption probability on these sites is modified by differences in the structural and chemical properties of the support and hence of the interface.

Acknowledgments

This work was supported by the Deutsche Forschungsgemeinschaft via Priority Programme SPP 1181 (BE 1201/13-2). We gratefully acknowledge J. Geserick (Institute of Inorganic Chemistry I, Ulm University) for preparing the mesoporous support materials, Dr. U. Hörmann, L. Kroner and C. Egger (Central Facility for Electron Microscopy, Institute of Micro- and Nanomaterials, Institute of Inorganic Chemistry I, Ulm University) for the TEM, XRD, and adsorption measurements, and G. Arnold (Center for Solar Energy and Hydrogen Research, Ulm) for the ICP-AES measurements.

References

[1] M. Haruta, T. Kobayashi, H. Sano, N. Yamada, Chem. Lett. (1987) 405.
[2] M. Haruta, CATECH 6 (2002) 102.
[3] G.C. Bond, C. Louis, D.T. Thompson, in: Catalysis by Gold, World Scientific, 1999.
[4] G.J. Hutchings, Gold Bull. 29 (1996) 123.
[5] M. Haruta, Catal. Surv. Jpn. 1 (1997) 61.
[6] D. Thompson, Gold Bull. 31 (1998) 111.
[7] G.C. Bond, D.T. Thompson, Gold Bull. 34 (2000) 117.
[8] M.C. Kung, R.J. Davis, H.H. Kung, J. Phys. Chem. C 111 (2007) 11767.
[9] G.C. Bond, C. Louis, D.T. Thompson, in: Catalysis by Gold, Imperial Press, London, 2007.
[10] D. Widmann, R. Leppelt, R.J. Behm, J. Catal. 251 (2007) 437.
[11] M. Kotobuki, R. Leppelt, D. Hansgen, D. Widmann, R.J. Behm, J. Catal. 264 (2009) 67.
[12] F. Boccuzzi, A. Chiorini, Stud. Surf. Sci. Catal. 140 (2001) 77.
[13] M.M. Schubert, S. Hackenberg, A.C. van Veen, M. Muhler, V. Plzak, R.J. Behm, J. Catal. 197 (2001) 113.
[14] C.K. Costello, M.C. Kung, H.-S. Oh, Y. Wang, H.H. Kung, Appl. Catal. A 232 (2002) 159.
[15] L.M. Molina, M.D. Rasmussen, B. Hammer, J. Chem. Phys. 120 (2004) 7673.
[16] S.H. Overbury, V. Schwartz, D.R. Mullins, W. Yan, S. Dai, J. Catal. 241 (2006) 56.
[17] J.J. Pietron, R.M. Stroud, D.R. Rolison, Nano Lett. 2 (2002) 545.
[18] S.H. Overbury, L. Ortiz-Soto, H. Zhu, B. Lee, M.D. Amiridis, S. Dai, Catal. Lett. 95 (2004) 99.
[19] J.-H. Liu, Y.-S. Chi, H.-P. Lin, C.-Y. Mou, B.-Z. Wan, Catal. Today 93–95 (2004) 141.
[20] C.-W. Chiang, A. Wang, B.-Z. Wan, C.-Y. Mou, J. Phys. Chem. B 109 (2005) 18042.
[21] C.-W. Chiang, A. Wang, C.-Y. Mou, Catal. Today 117 (2007) 220.
[22] Y. Denkwitz, J. Geserick, U. Hörmann, V. Plzak, U. Kaiser, N. Hüsing, R.J. Behm, Catal. Lett. 119 (2007) 199.
[23] K.Y. Ho, K.L. Yeung, Gold Bull. 40 (2007) 15.
[24] D. Wang, Z.D.S. Ma, J. Liu, Z. Nie, M.H. Engelhard, Q. Huo, C. Wang, R. Kou, J. Phys. Chem. C 112 (2008) 13499.
[25] Y. Zhu, W. Li, Y. Zhou, X. Lu, X. Feng, Z. Yang, Catal. Lett. 127 (2009) 406.
[26] Y. Denkwitz, M. Makosch, J. Geserick, U. Hörmann, S. Selve, U. Kaiser, N. Hüsing, R.J. Behm, Appl. Catal. B: Environ. (2009), doi:10.1016/j.apcatb.2009.06.016.
[27] J. Geserick, N. Hüsing, R. Rosmanith, K. Landfester, C.K. Weiss, Y. Denkwitz, R.J. Behm, U. Hörmann, U. Kaiser, Mesoporous Silica and Titania by Glycol-modified Precursors, 2006, 1007, Materials Research Society, Boston, 2006. p. S04-13.
[28] R. Leppelt, D. Hansgen, D. Widmann, T. Häring, G. Bräth, R.J. Behm, Rev. Sci. Instrum. 78 (2007) 104103.
[29] V. Plzak, J. Garche, R.J. Behm, European Fuel Cell News 10 (2003) 16.
[30] B. Schumacher, V. Plzak, J. Cai, R.J. Behm, Catal. Lett. 101 (2004) 215.
[31] R. Zanella, C. Louis, Catal. Today 107–108 (2005) 768.
[32] In a few cases, a different drying procedure was used, by drying the catalyst in vacuum for 15 h at 100 °C. This led to similar results as drying in an Ar stream.
[33] Note that this pre-treatment procedure is slightly different from that used in Ref. [11]. In the previous experiments, the catalyst was calcined *ex-situ*, in a separate reactor, which allows for interaction with H_2O and CO_2 during sample transfer into the TAP reactor. This is ruled out in the present experiments.
[34] J.F. Moulder, W.F. Stickle, P.E. Sobol, K.D. Bomben, in: Handbook of X-ray Photoelectron Spectroscopy, Perkin Elmer Corp., Eden Prairie/USA, 1992.
[35] H.-G. Boyen, G. Kästle, F. Weigl, B. Koslowski, C. Dietrich, P. Ziemann, J.P. Spatz, S. Riethmüller, C. Hartmann, M. Möller, G. Schmid, M.G. Garnier, P. Oelhafen, Science 297 (2002) 1533.
[36] J.T. Gleaves, J.R. Ebner, T.C. Kuechler, Catal. Rev. Sci. Eng. 30 (1988) 49.
[37] S.O. Shekhtman, G.S. Yablonsky, S. Chen, J.T. Gleaves, Chem. Eng. Sci. 54 (1999) 4371.